

OBSERVATION OF SPIN 1 $f_1(1285)$ IN THE REACTION
 $\gamma\gamma^* \rightarrow \eta^0\pi^+\pi^-$

G. Gidal, J. Boyer, F. Butler, D. Cords, G.S. Abrams, D. Amidei^a, A.R. Baden, T. Barklow, A.M. Boyarski, P. Burchat^b, D.L. Burke, J.M. Dorfan, G.J. Feldman, L. Gladney^c, M.S. Gold, G. Goldhaber, L.J. Golding^d, J. Haggerty^e, G. Hanson, K. Hayes, D. Herrup, R.J. Hollebeek^c, W.R. Innes, J.A. Jaros, I. Juricic, J.A. Kadyk, D. Karlen, S.R. Klein, A.J. Lankford, R.R. Larsen, B.W. LeClaire, M.E. Levi, N.S. Lockyer^c, V. Lüth, C. Matteuzzi^f, M.E. Nelson^g, R.A. Ong, M.L. Perl, B. Richter, K. Riles, P.C. Rowson^h, T. Schaadⁱ, H. Schellman^a, W.B. Schmidke, P.D. Sheldon^j, G.H. Trilling, C. de la Vaissière^k, D.R. Wood, J.M. Yelton^l, and C. Zaiser

*Lawrence Berkeley Laboratory and Department of Physics
University of California, Berkeley, California 94720*

*Stanford Linear Accelerator Center
Stanford University, Stanford, California 94305*

*Department of Physics
Harvard University, Cambridge, Massachusetts 02138*

Abstract

We observe both the $J^{PC} = 1^{++} f_1(1285)$ and the $J^{PC} = 0^{-+} \eta'(958)$ in tagged two photon interactions and the $\eta'(958)$ in untagged interactions. The measured Q^2 dependence and decay distribution support the $f_1(1285)$ spin-parity assignment. The radiative width of the $f_1(1285)$ is measured as $\frac{M^2}{Q^2} \cdot \Gamma_{\gamma\gamma^*} = 8.2 \pm 2.2 \pm 1.5$ keV, assuming a ρ -pole form factor.

Submitted for Publication

[†]This work was supported in part by the Department of Energy under contracts DE-AC03-76SF00098, DE-AC03-76SF00515, and DE-AC02-76ER03064.

^aPresent address: University of Chicago, Chicago, IL 60637

^bPresent address: University of California, Santa Cruz, CA 95064

^cPresent address: University of Pennsylvania, Philadelphia, PA 19104

^dPresent address: Therma-Wave Corporation, Fremont, CA 94539

^ePresent address: Brookhaven National Laboratory, Upton, NY 11973

^fPresent address: CERN, CH-1211 Geneva 23, Switzerland

^gPresent address: California Institute of Technology, Pasadena, CA 91125

^hPresent address: Columbia University, New York, NY 10027

ⁱPresent address: University of Geneva, CH-1211 Geneva 4, Switzerland

^jPresent address: University of Illinois, Urbana, IL 61801

^kPresent address: LPNHE, Univ. Pierre Marie Curie, Paris, France F-75230

^lPresent address: Oxford University, Oxford, England

The recent observation^{(1),(2)} of a spin-1 resonance in the $K\bar{K}\pi$ final state produced in $\gamma\gamma^*$ interactions encourages a similar search in other final states. The large radiative width observed for this $K\bar{K}\pi$ resonance puts into question its association with the $f_1(1420)$ in an ideally mixed $J^{PC} = 1^{++}$ nonet. It would thus be interesting to observe the production of other members of the nonet to establish a consistent picture.

We report here on a study of the reaction

$$e^+e^- \rightarrow e^+e^-\eta^0\pi^+\pi^- \quad (1)$$

with both tagged and untagged final state electrons. The η^0 is identified through its decay into two photons. The results are based on an integrated luminosity of 220 pb^{-1} obtained with the Mark II detector at the PEP electron-positron storage rings, run at a center of mass energy of 29 GeV.

The major features of the Mark II detector have been well described elsewhere.⁽³⁾ We comment here only on those aspects particularly relevant to this study. The position and energy of the photons are measured in the eight liquid-argon barrel calorimeter modules which subtend 64% of the solid angle and have an energy resolution of $0.14/\sqrt{E(\text{GeV})}$ and an angular resolution of 15 mrad. The proportional chamber endcap calorimeters are primarily used to veto events with extra photons. The relatively low 2.3 kG solenoidal magnetic field was especially useful in permitting low p_T pions to reach the time of flight counters and hence trigger the detector. The inner vertex chamber allowed accurate measurement of these tracks, with a precision $\Delta p/p = [(0.025)^2 + (0.01p(\text{GeV}))^2]^{\frac{1}{2}}$, compensating for the low magnetic field. The small angle tagging system (SAT) measures scattered

electrons between 21 and 83 mrad from the beam direction. The SAT consists of three sets of four planar drift chambers for tracking and an electromagnetic shower counter to identify the scattered electron and measure its energy. Each set of drift chambers is arranged in a rectangular array around the beam pipe so that maximum efficiency is obtained in the corner overlap regions. The octagonal shower counters consist of 18 alternating layers of $\frac{1}{4}$ " Pb and $\frac{1}{2}$ " scintillator with the light from the first five and last 13 layers separately collected in wave-shifter bars at one end. The energy scale is calibrated with Bhabhas, and the measured energy resolution is $\Delta E/E = 15.5\%/\sqrt{E(\text{GeV})}$.

We select events with two oppositely charged tracks and at least two photons in the central detector. The photons are required to be well isolated from both charged tracks and other photons and to have a measured energy greater than 200 MeV. Events with more than two gammas are also considered because the reconstruction program and hadronic interactions can create apparent extra photons. Events which also have one good track with more than 7 GeV in the SAT counters are referred to as tagged ($\gamma\gamma^*$) events. The tagging angular interval gives good acceptance for a four momentum transfer, Q^2 , interval of 0.15 to 1.2 (GeV/c)². The measured gamma-gamma invariant mass shows a clear π^0 peak but the η^0 is submerged in combinatorial background. To choose η^0 candidates and minimize the combinatorial background we require that this measured $\gamma\gamma$ mass lie between 0.45 and 0.75 GeV. Pairs of photons are then constrained to the η^0 mass and a chi-squared < 5.0 is required in the fit. After the η^0 selection the events are checked for remaining extra gammas that are not obviously associated with charged or neutral tracks. Events having such extra gammas are taken as a measure of the background.

The sum of the transverse momenta (Σp_T) is calculated, and, for untagged ($\gamma\gamma$) events, the $|\Sigma p_T|$ is required to be less than 200 MeV/c. Because of the increased measurement error of the tagging electron, we open this cut to 400 MeV/c for tagged events.

In Figure 1 we show the $\eta^0\pi^+\pi^-$ mass distribution for the untagged event sample. There is a clear peak at the $\eta'(958)$ but no other narrow structure is seen. The Σp_T distribution for the $\eta'(958)$ mass region is in excellent agreement with Monte Carlo simulations. The higher mass continuum region is believed to be background, dominated by feeddown from higher multiplicity $\gamma\gamma$ interactions, as evidenced by the broader Σp_T distribution in this region. A Gaussian fit to the η' mass and width gives $m_{\eta'} = 956.3 \pm 1.0$ MeV, in reasonable agreement with the accepted mass⁽⁴⁾ within our present understanding of the systematic errors. The width, $\sigma = 9 \pm 1$ MeV, is consistent with the detector resolution as determined by the Monte Carlo simulations. The 143 ± 12 events above background, corrected for efficiency and unseen decay modes correspond to a cross section $\sigma(e^+e^- \rightarrow e^+e^-\eta') = 1.52 \pm 0.19 \pm 0.30$ nb. The cross section for production of a narrow resonance R with $J = 0$ in the equivalent photon approximation is,⁽⁵⁾ with $\tau = M_R^2/s$,

$$\sigma_{e^+e^- \rightarrow e^+e^-R} = \left(\frac{\alpha}{\pi}\right)^2 \left[\ln\left(\frac{s}{4m_e^2}\right) \right]^2 \cdot \frac{8\pi^2\Gamma(R \rightarrow \gamma\gamma)}{M_R^3} \cdot G(\tau) \cdot C_1(\tau) \quad (2)$$

where $G(\tau) \equiv (1 + \tau/2)^2 \ln(1/\tau) - \frac{1}{2}(1 - \tau)(3 + \tau)$, and $C_1(\tau) = 0.78$ is the ratio of the exact $\gamma\gamma$ luminosity to that obtained in the leading log approximation, giving a measured radiative width $\Gamma(\eta'(958) \rightarrow \gamma\gamma) = 4.7 \pm 0.6 \pm 0.9$ keV. This agrees with the current world average⁽⁶⁾ of 4.3 ± 0.3 keV based almost entirely on measurements that use the $\rho^0\gamma$ decay mode of the $\eta'(958)$.

In Figure 2a we show the $\eta^0\pi^+\pi^-$ invariant mass distribution for the tagged events.

The $\eta(958)$ signal remains, but now we clearly see an additional narrow signal above background at a mass of 1286 ± 9 MeV and with a $\sigma = 26 \pm 5$ MeV. This second peak can be identified with the $f_1(1285)$ or the $\eta(1275)$,⁽⁷⁾ or both. The absence of such a signal in the untagged sample (Figure 1) can be used to set a limit of $B(R(1285) \rightarrow \eta\pi\pi) \cdot \Gamma(R(1285) \rightarrow \gamma\gamma) < 0.62$ keV (95% C.L.). Since spin-1 production is not allowed for real photon-photon collisions while spin-0 production should be even more prominent, we identify the signal in the tagged events primarily with the spin-1 $f_1(1285)$. We can expect to enhance the signal with respect to background by removing events at small four momentum transfer, Q^2 . Figure 2b shows the same $\eta^0\pi^+\pi^-$ mass plot for those events with $Q^2 > 0.2$ (GeV/c)² and shows the expected effect. The $\eta\pi^+\pi^-$ mass plot for those events which otherwise satisfy the selection criteria but which were ultimately removed because they contained extra photons, is shown in Figure 2c. These events are again presumed to be a feiddown from higher multiplicity $\gamma\gamma^*$ interactions as indicated by their Σp_T distribution. The mass distribution is structureless and resembles the overall background in Figures 2a and 2b. Since the $f_1(1285)$ is expected to decay primarily via $a_0(980)\pi$, we also show, in Figure 2d, the same $\eta\pi^+\pi^-$ mass distribution requiring that one $\eta\pi^\pm$ mass combination lie between 0.90 and 1.06 GeV. Again a prominent peak remains, but the limited phase space allows no definite statement concerning the presence of $a_0(980)$. Monte Carlo simulations of $\gamma\gamma^* \rightarrow f_1(1285) \rightarrow a_0(980)\pi \rightarrow \eta\pi^+\pi^-$ are used to calculate the efficiency giving $\sigma(e^+e^- \rightarrow e^+e^- f_1(1285)) \cdot B(f_1(1285) \rightarrow \eta\pi\pi) = 27.6 \pm 7.4 \pm 4.1$ pb for the Q^2 interval between 0.2 and 1.2 (GeV/c)²

For the spin-1 case, the formula comparable to (2) has recently been given by Cahn⁽⁸⁾

as

$$\begin{aligned}
\sigma(e^+e^- \rightarrow e^+e^-R) = & 2 \left(\frac{\alpha}{2\pi}\right)^2 \ln\left(\frac{s}{4m_e^2}\right) \cdot \frac{16\pi^2}{M_R^3} \cdot \frac{3}{2} \tilde{\Gamma}_{R\gamma\gamma^*} \cdot C_2(\tau) \\
& \times \left\{ 4[(1+\tau) \ln 1/\tau - (1-\tau)(7/4 + \tau/4)] \int \frac{dQ^2}{M_R^2} \cdot F(Q^2)^2 \right. \\
& \left. + \frac{1}{2} \cdot 4 \left[(1+\tau/2)^2 \ln(1/\tau) - \frac{1}{2}(1-\tau)(3+\tau) \right] \int \frac{dQ^2}{M_R^2} \cdot \frac{Q^2}{M_R^2} \cdot F(Q^2)^2 \right\} \quad (3)
\end{aligned}$$

where $\tilde{\Gamma} \equiv \frac{M^2}{Q^2} \Gamma$ in the low Q^2 limit and the residual Q^2 dependence is contained in a form factor taken as $F(Q^2) = \frac{1}{1+Q^2/m_\rho^2}$. The factor $C_2(\tau) = 0.91$ is again the ratio of the exact $\gamma\gamma^*$ luminosity to that used in reference (8). For a branching ratio $B(f_1(1285) \rightarrow \eta\pi\pi) = 0.49$ and $m_\rho = 0.76$ GeV the measured cross section together with equation (3) evaluated for $\sqrt{s} = 29$ GeV and $M_R = 1.285$ GeV gives $\tilde{\Gamma}(f_1(1285) \rightarrow \gamma\gamma^*) = 8.2 \pm 2.2 \pm 1.5$ keV. It is important to note that this result is rather sensitive to the assumed Q^2 dependence of the form factor.

In Figure 3 we show the value of $\tilde{\Gamma}_{\gamma\gamma^*}$ for the $f_1(1285)$ obtained in two intervals of Q^2 . The similarity of the two values indicates that the Q^2 dependence of the data is consistent with the form assumed in equation (3). We also show the Q^2 dependence of $\Gamma_{\gamma\gamma^*}$ for the spin-0 $\eta'(958)$ as inferred from⁽⁹⁾

$$\sigma_{e^+e^- \rightarrow e^+e^-\eta'} = \left(\frac{\alpha}{\pi}\right)^2 \ln\left(\frac{s}{4m_e^2}\right) G(\tau) \cdot C_3(\tau) \cdot \Gamma_{\gamma\gamma^*} \cdot \frac{8\pi^2}{M^3} \int (1+Q^2/M^2) F^2(Q^2) \frac{dQ^2}{Q^2}.$$

Again, the radiative widths are consistent with the assumed form. In the same figure, we also show the upper limit on $\Gamma_{\gamma\gamma^*}$ obtained above for the $f_1(1285)$ assuming it were spin-0.

Cahn⁽⁸⁾ has also pointed out that for small Q^2/M^2 , the distribution in the angle θ between the normal to the decay plane and the incident photon, in the rest frame of the produced resonance, is proportional to $\sin^2 \theta$ for a 1^- particle and $1 + \cos^2 \theta$ for a

1^{++} particle. Monte Carlo studies indicate that the resolution in $\cos \theta$ is approximately $\sigma(\cos \theta) = 0.05$. This measured distribution in $|\cos \theta|$ is shown in Figure 4 for the 31 events in Figure 2b between 1.22 and 1.34 GeV/c², normalized to the Monte Carlo simulation. The experimental distribution expected⁽¹⁰⁾ for a 1^{++} resonance is a better fit ($\chi^2 = 2.5$) than the distribution expected for a 1^{-+} resonance ($\chi^2 = 10.0$).

Renard⁽¹¹⁾ and Cahn⁽⁸⁾ have estimated the $\gamma\gamma^*$ width of the usual $1^{++}q\bar{q}$ nonet with ideal mixing in a nonrelativistic quark model and, based on the observed width $\Gamma(f_2(1270) \rightarrow \gamma\gamma) = 2.7$ keV, predict $\tilde{\Gamma}(f_1(1285) \rightarrow \gamma\gamma^*) = 4.5$ keV, in reasonable agreement with our measurement. If the nonet deviates from ideal mixing with the quark composition of the $f_1(1420)$ taken to be $\cos \lambda |s\bar{s}\rangle - \sin \lambda |(u\bar{u} + d\bar{d})/\sqrt{2}\rangle$, then a value $\lambda = -14^{+5}_{-10}^\circ$ can accommodate the observed ratio⁽²⁾ $\Gamma(f_1(1285) \rightarrow \gamma\gamma^*)/\Gamma(f_1(1420) \rightarrow \gamma\gamma^*) = 3.0 \pm 1.6$.

Chanowitz⁽¹²⁾ has also pointed out that a substantial deviation from ideal mixing would predict $\eta\pi\pi$ signals for both the $f_1(1285)$ and $f_1(1420)$ mesons. There is evidence⁽²⁾ that the peak observed at 1420 MeV favors a $K^*\bar{K}$ decay rather than an $a_0(980)\pi$ decay. If the $a_0(980)\pi$ decay mode were important, or if there were an independent $\eta\pi\pi$ decay, we would expect to see a signal at 1420 MeV in Figure 2b. No such $\eta\pi\pi$ signal is seen and we can give an upper limit $B(R(1420) \rightarrow \eta\pi\pi) \cdot \tilde{\Gamma}(R(1420) \rightarrow \gamma\gamma^*) < 1.5$ keV (95% C.L.). Comparing this limit to our measurement⁽²⁾ of this product for the $K\bar{K}\pi$ decay mode gives $B(R(1420) \rightarrow \eta\pi\pi)/B(R(1420) \rightarrow K\bar{K}\pi) < 0.56^{+.44}_{-.18}$.

In summary, we have observed the $f_1(1285)$ and the $\eta'(958)$ in the $\eta\pi^+\pi^-$ final state produced in tagged photon-photon interactions as well as the $\eta'(958)$ in untagged interac-

tions. The absence of $f_1(1285)$ production at very small Q^2 and its decay distribution at finite Q^2 support the $J^{PC} = 1^{++}$ assignment.

We gratefully acknowledge the significant collaboration of R.N. Cahn and helpful discussions with M.S. Chanowitz and J. Smith.

References

- (1) A. Aihara et al., Phys. Rev. Lett. 57 (1986) 2500.
- (2) G. Gidal et al., LBL-22691 (submitted to Phys. Rev. Lett.); A preliminary version of these results was presented in Proceedings of the 23rd International Conference on High Energy Physics, Berkeley, California, July 1986 (World Scientific).
- (3) R.H. Schindler et al., Phys. Rev. D24 (1981) 78; G.S. Abrams et al., IEEE Trans. Nucl. Sci. 27 (1980) 59; J. Smith, Ph.D. Thesis, University of California, Davis, 1983.
- (4) Review of Particle Properties, Phys. Lett. 170B (1986) 1.
- (5) F. Low, Phys. Rev. 120 (1960) 582. For luminosity corrections see J.H. Field, Nucl. Phys. B168 (1980) 477; Erratum, Nucl. Phys. B176 (1980) 545.
- (6) B. Shen, VIIth International Workshop on Photon-Photon Collisions, Paris, France, April 1-5, 1986.
- (7) N. Stanton et al., Phys. Rev. Lett. 42 (1979) 346; A. Ando et al., Phys. Rev. Lett. 57 (1986) 1296.
- (8) R.N. Cahn, Production of Spin-One Resonances in $\gamma\gamma^*$ Collisions, LBL-22555 (submitted for publication). This paper also shows that the formalism agrees with the more traditional formulation of V.M. Budnev et al., Phys. Reports 15 (1975) 181.
- (9) R.N. Cahn, private communication.

- (10) The expected angular distributions have been corrected for the finite Q^2 interval sampled, to order Q^2/M^2 (J. Boyer and R.N. Cahn, private communication).
- (11) F.M. Renard, Nuovo Cimento 80A (1984) 1.
- (12) M.S. Chanowitz, An Exotic Quark-Gluon Hybrid at 1420 MeV?, LBL-22611, December 1986 (submitted for publication).

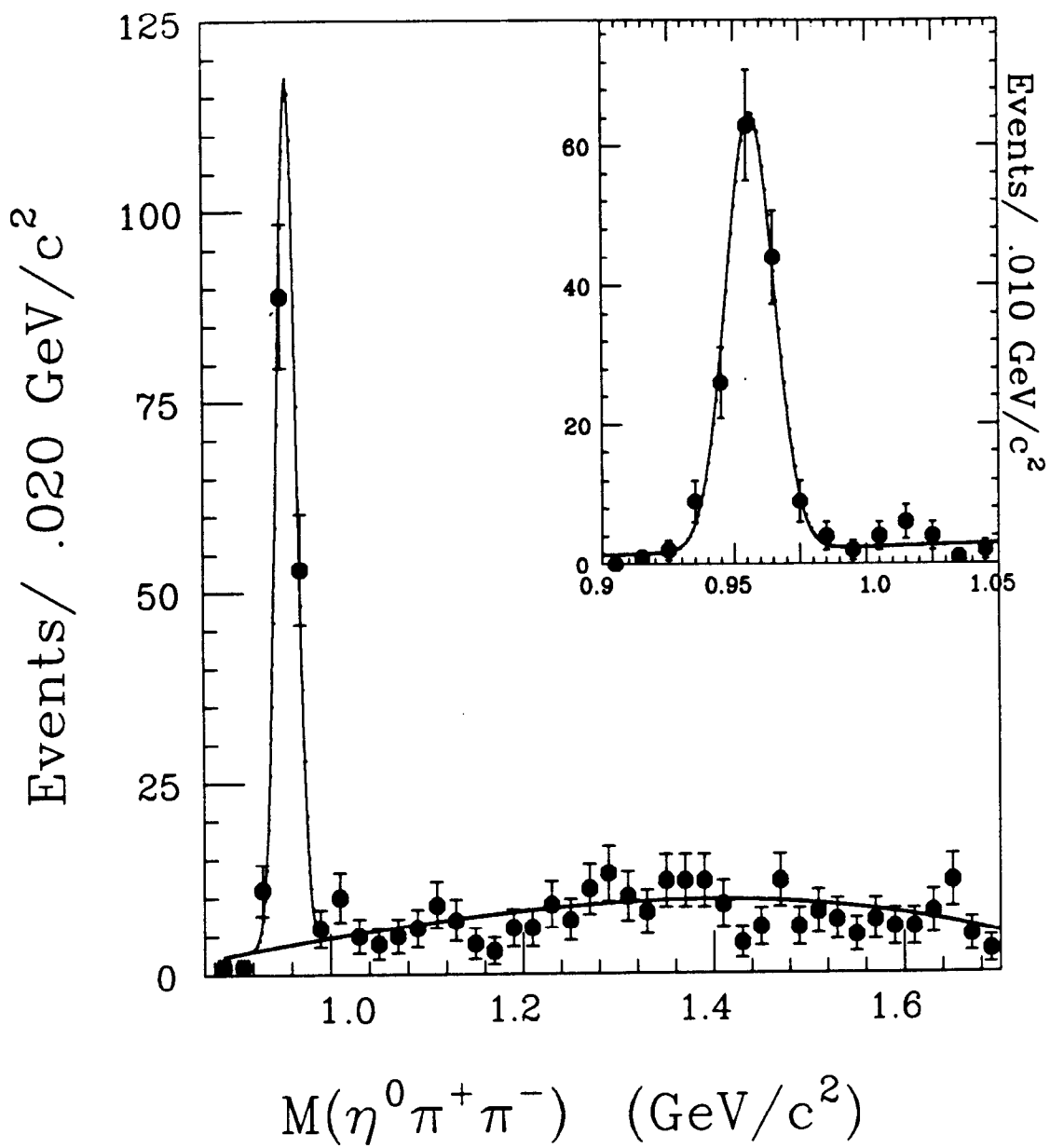
Figure Captions

Fig. 1 The $\eta^0\pi^+\pi^-$ invariant mass for untagged events with no extra gammas. The solid curve is the result of a fit to a Gaussian and a polynomial background.

Fig. 2 The $\eta^0\pi^+\pi^-$ invariant mass for (a) all tagged events without extra gammas; (b) those events with $Q^2 > 0.2$ (GeV/c^2); (c) events with extra gammas; and (d) events in (b) which also have $0.90 < m(\eta^0\pi^\pm) < 1.06$ GeV/c^2 .

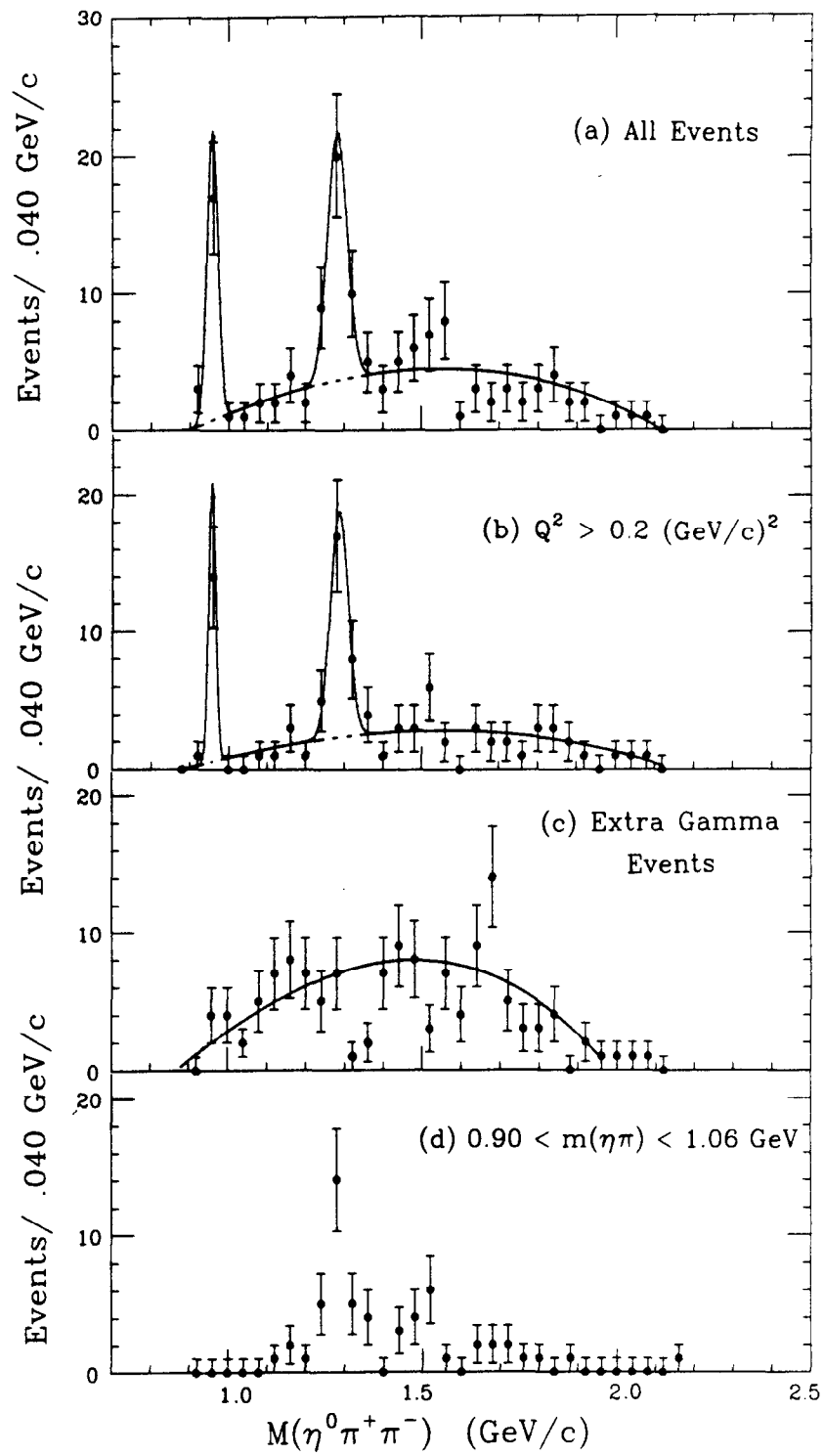
Fig. 3 The Q^2 dependence of the radiative widths of the $J = 1$ $f_1(1285)$ and the $J = 0$ $\eta'(958)$. We also show the 95% confidence level upper limit for a $J = 0$ $R(1285)$ near $Q^2 = 0$. A ρ -pole form factor is assumed in each case.

Fig. 4 The measured distribution in $|\cos\theta|$ for the $f_1(1285)$, where θ is the decay angle defined in the text. The solid (dashed) histograms are the result of Monte Carlo simulations of the distributions expected for $J^{PC} = 1^{++}$ ($J^{PC} = 1^{-+}$).



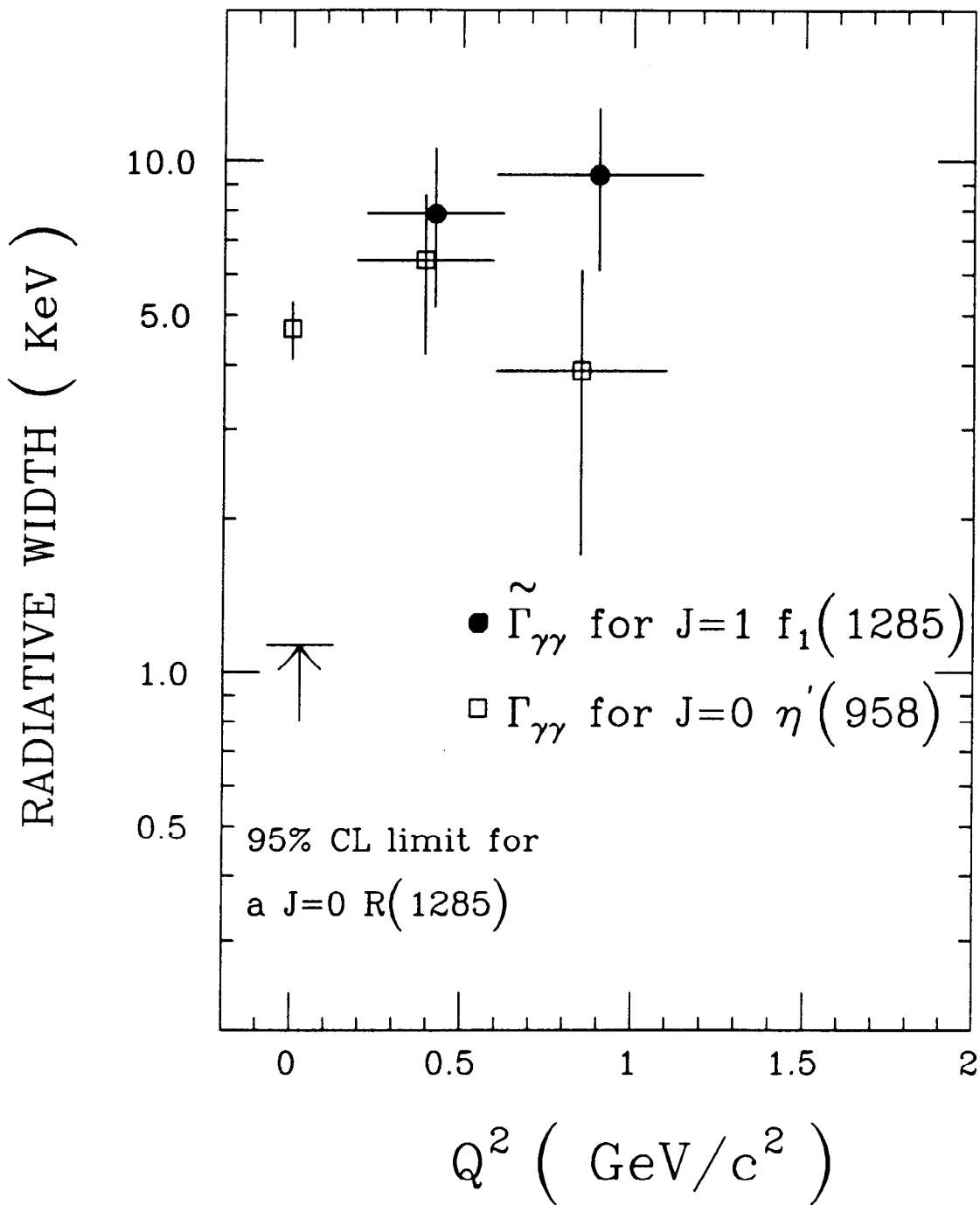
XBL 874-1767

Figure 1



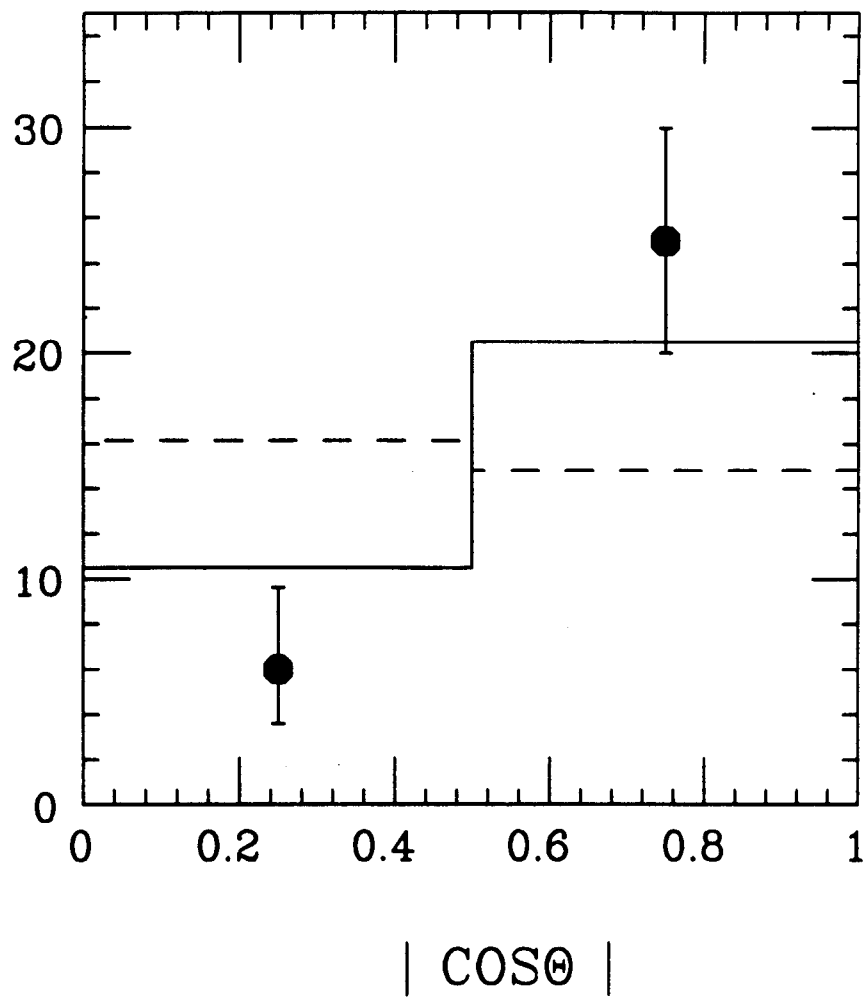
XBL 874-1774

Figure 2



XBL 874-1768

Figure 3



XBL 874-1770

Figure 4